Published in final edited form as:
Nat Neurosci. 2017 June ; 20(6): 845–853. doi:10.1038/nn.4543.

Sharp wave ripples during learning stabilize hippocampal spatial map

Lisa Roux[1], **Bo Hu**[1], **Ronny Eichler**[1], **Eran Stark**[1,2], and **György Buzsáki**[1,3,4,*]

[1]New York University Neuroscience Institute, New York University, New York, New York 10016, United States of America

[2]Tel Aviv University, Sackler Faculty of Medicine and Sagol School of Neuroscience, Department of Physiology and Pharmacology, Tel Aviv, Israel

[3]Department of Neurology, Medical Center, New York University, New York, New York 10016, United States of America

[4]Center for Neural Science, New York University, New York, New York 10016, United States of America

Abstract

Cognitive representation of the environment requires a stable hippocampal map but the mechanisms maintaining map representation are unknown. Because sharp wave-ripples (SPW-R) orchestrate both retrospective and prospective spatial information, we hypothesized that disrupting neuronal activity during SPW-Rs affects spatial representation. Mice learned daily a new set of three goal locations on a multi-well maze. We used closed-loop SPW-R detection at goal locations to trigger optogenetic silencing of a subset of CA1 pyramidal neurons. Control place cells (non-silenced or silenced outside SPW-Rs) largely maintained the location of their place fields after learning and showed increased spatial information content. In contrast, the place fields of SPW-R-silenced place cells remapped, and their spatial information remained unaltered. SPW-R silencing did not impact the firing rates or the proportions of place cells. These results suggest that interference with SPW-R-associated activity during learning prevents the stabilization and refinement of the hippocampal map.

Introduction

During exploration of an environment, hippocampal place cells fire selectively in particular locations1 (their “place fields”) and the sequential activation of groups of place fields can reliably describe the trajectory of the animal2. Collectively, a map-like representation built from place cells may serve a cognitive navigation mechanism1,3. Remarkably, entire place

*Corresponding author: gyorgy.buzsaki@nyumc.org.
Present address: B. Hu Third Military Medical University, College of Basic Medical Sciences, Department of Physiology, Chongqing, China
Present address: R. Eichler Radboud University Nijmegen, Donders Centre for Neuroscience, Departments of Neuroinformatics and Neurophysiology, Nijmegen, Netherlands

cell sequences activated during exploration are repeated or “replayed” during sharp wave ripple complexes (SPW-Rs), a network event observed in the hippocampal local field potential4 during non-REM sleep5–8 and transient immobility periods of waking exploration9–16. It has been hypothesized that SPW-R-related replay of place cell sequences in the hippocampus mediates memory consolidation and transfer of learned information from the hippocampus to the neocortex for long-term storage17–19. In support of this memory consolidation framework, experiments show that selectively interfering with SPW-Rs during sleep deteriorates memory performance20,21 and recently formed spatial representations22 (but see23). During wakefulness, SPW-Rs may have different functions. They are thought to help constructing cognitive maps of the physical world12,24,25 and are involved in the planning of future routes11,12,14–16 (“prospective” function). Disruption of awake SPW-Rs also impairs behavioral performance13. Despite these findings, the relationship between awake SPW-Rs, hippocampal maps and memory consolidation remains to be clarified.

Mental navigation and spatial navigation are believed to be supported by similar neurophysiological mechanisms26. During learning and retrieval, memories are known to be transiently labile27 and thus require a subsequent stabilization process17,28. Therefore, the question arises whether spatial representations (like memories) also need to be “stabilized”. Recent experiments suggest that indeed, active neuronal processes support hippocampal map stabilization as optogenetic silencing of hippocampal neurons during exploration29 or during SPW-R of sleep22 affects place field stability. Yet, the neurophysiological mechanisms supporting the stabilization of the hippocampal map upon learning are still unknown.

We hypothesized that SPW-Rs are instrumental in stabilizing the spatial representation coded by place cells in the CA1 region of the hippocampus during learning. To examine the role of SPW-Rs in place field stabilization, we used focal optogenetic silencing of a subset of pyramidal neurons during SPW-Rs in a hippocampus-dependent spatial memory task30. The stability of the silenced place cells was compared with those of simultaneously recorded but non-silenced place cells and place cells silenced after SPW-Rs with a random delay. The spatial correlates of control place cells were largely maintained and showed an increased spatial information content after learning. In contrast, the place fields of SPW-R-silenced neurons drifted and their information failed to increase. Our findings support the hypothesis that SPW-R-associated neuronal activity is necessary for stabilizing and refining hippocampal place fields and, by extension, for maintaining a stable cognitive map.

Results

Closed-loop focal optogenetic silencing of place cells

Mice (n = 5; four CaMKII-Cre::Arch and one PV-Cre::ChR2; Supplementary Fig. 1 and 2) were trained in a spatial learning task30 (Fig. 1). After pre-training (3 to 4 days), they were implanted with silicon probes in the CA1 region (Supplementary Fig. 1b-c) and recorded during free behavior in their home cage or while performing on a “cheeseboard” maze. Mice carried two LEDs (Fig. 1b), which allowed monitoring their exact location in real-time. Each session consisted of five stages (Fig. 1a). During the learning epoch, the mouse performed

multiple trials (29 – 60 trials/session; median 50; n = 29 sessions; Supplementary Table 1) on the cheeseboard maze, where it had to find the locations of three goal wells (baited with hidden water rewards) out of 177 possible wells. A trial was completed once the mouse had retrieved all rewards and returned to the start box to collect an additional water reward (Fig. 1c). The locations of the goal wells changed every day but were fixed within a day. This strategy required the mice to daily update their memory for the new goal locations in a familiar environment. Immediately before and after training, the mouse was placed back in its home cage and allowed to sleep for approximately 1 h. Memory performance and place field properties were assessed during pre- and post-learning exploration epochs during which the mouse was allowed to explore the maze for 30 minutes. No rewards were available during the first 10 min, after which water drops were placed in several randomly selected wells to encourage exploration of the entire platform (online Methods). Similar to rats30, daily learning was rapid, and the mice developed stereotyped and efficient trajectories after 5-10 trials (Fig. 1c). Memory of the newly learned goal locations was also demonstrated by the fact that mice spent significantly more time at the goal locations during the first 10 minutes of the post-learning epoch compared to pre-learning epoch (Fig. 1d; $P = 0.0006$; n = 29 sessions; Wilcoxon's paired signed rank test).

During the learning epoch of the task, SPW-Rs occurred regularly at the goal locations while the animal was collecting rewards30 (Fig. 2d). We hypothesized that these SPW-Rs shape the spatial representation coded by place cells in this learning paradigm. To test the impact of the SPW-Rs on CA1 hippocampal place fields, we used closed-loop optogenetic silencing of pyramidal cells, contingent upon real-time detection of spontaneous SPW-Rs at the goal locations. Importantly, optogenetic suppression of pyramidal neuronal activity was conducted in a focal manner so that both light-responsive and control neurons could be simultaneously recorded and compared, without impacting the overall hippocampus function. To deliver light focally, the recording silicon probes were equipped with etched optical fibers coupled to head-mounted laser diodes31 (one fiber per shank; Fig. 2a-c) and implanted in one (n = 2) or both (n = 3 mice) hemispheres (Supplementary Fig. 1a). During the first rest period, we characterized the effect of light on the firing rate of each recorded neuron (100 ms light pulses; 300 pulses at 0.2Hz; 204 ± 30 μW, mean ± SEM; online Methods). For each neuron, we defined a light-response index by comparing spiking activity between the light pulses and the preceding baseline periods (100ms intervals starting 1 s before stimuli onset) to define a light-response index (Fig. 2c; Supplementary Fig. 3 and 4; online Methods). In both CaMKII-cre::Arch (direct suppression; Fig. 2b) and PV-cre::ChR2 mice (indirect suppression; Supplementary Fig. 5), focal illumination silenced most pyramidal cells recorded on the illuminated shank and occasionally some on neighboring shanks (Fig. 2c). Of the 1020 putative pyramidal cells that we recorded, 402 were significantly suppressed ($P < 0.05$; Wilcoxon's paired signed rank tests; online Methods).

During the learning epoch, light stimuli (60 ms pulses; same light intensity as during response characterization) were triggered by online detection of spontaneous SPW-Rs to focally suppress firing of pyramidal neurons and terminate SPW-R oscillations31 ("ripple-locked" paradigm; Fig. 2d-e; n = 22 recording sessions). This SPW-R-contingent silencing of pyramidal neurons was confined to events occurring when head of the mouse was within the goal area by means of real time position tracking (Fig. 2d, green circles). Our SPW-R

manipulation was mainly restricted to the second half of the SPW-Rs31 (Supplementary Fig. 6). Yet, optogenetic stimulation was effective at targeting most SPW-Rs during immobility periods (82 ± 4 %; online Methods). To test for potential effects of light stimulation, not-specific to SPW-R silencing, light stimuli were also delivered with a delay (100-300ms; 60 ms pulses) relative to SPW-R detection ("ripple-delayed" paradigm), either in separate recording sessions (n = 7 sessions) or in combination with the ripple-locked paradigm but in the opposite hemisphere (n = 9 sessions). The behavioral performance (measured by the proportion of time spent in goal areas in the post-learning exploration compared to the pre-learning exploration epoch; Fig. 1d) was identical regardless of whether a ripple-locked or a ripple-delayed paradigm was employed during the learning task (P = 0.7; Mann-Whitney U test on the differences Post - Pre; n = 7 ripple-delayed and n = 13 ripple-locked sessions; Supplementary Fig. 7).

Of the 1406 units recorded in 29 sessions, 227 were classified as putative interneurons and 1020 as putative pyramidal cells (online Methods; Supplementary Fig. 3a). Of the putative pyramidal cells, 637 had a place field on the cheeseboard maze in a least one of the two exploration epochs (pre- and post-learning; online Methods). For quantitative analyses, we used two approaches. (1) In the first approach, place cells that were silenced by light pulses in the ripple-locked paradigm were referred to as *silenced*, whereas place cells silenced in the ripple-delayed paradigm are referred to as *delayed*. Place cells that were unaffected by light pulses in both of these stimulation paradigms were defined as *control* (Fig. 2f-g). Of the 637 place cells, 106 were discarded because they did not meet our criteria for classification (online Methods; Supplementary Table 1). Of the 531 remaining place cells, 167 were assigned to the *silenced*, 81 to the *delayed* silenced and 283 the *control* groups (Fig. 2g). (2) Because silencing of pyramidal neurons may bring about local circuit effects3, we also used an alternative categorization, in which we grouped place cells based on the type of intervention done (ripple-locked versus ripple-delayed paradigms), independently of the magnitude of their responses to light. The two groups in this second approach were referred to as *ripple-locked* and *ripple-delayed* place cells (n = 385 and n = 247 place cells, respectively).

Perturbation of SPW-R-associated neuronal activity destabilizes place fields

Stability of the hippocampal spatial map was examined by comparing recordings from the pre-learning and post-learning exploration epochs in the *control*, *silenced* and *delayed* groups of place cells. No light stimulation was administered during these epochs. Figure 3a-c illustrates representative rate maps for *control*, *silenced* and *delayed* place cells. For each place cell, we calculated the pixel-by-pixel Pearson correlation coefficient between the rate maps obtained from the pre- and post-learning epochs to quantify the stability of the spatial representation. By comparing the resulting correlation coefficients across the *control*, *silenced* and *delayed* groups, we found that optogenetic silencing of pyramidal neurons during SPW-Rs reduced the stability of the rate map compared to control neurons (Fig. 3d). In contrast, delayed suppression of place cells had no consistent effect (mean correlation coefficient ± SEM: 0.56 ± 0.02; 0.60 ± 0.03 and 0.49 ± 0.02 for *control*, *delayed* and *silenced* ensembles, respectively; overall group effect, Kruskall Wallis test, P = 0.002; Tukey's post-hoc tests, *silenced* vs *control*, P = 0.008; *silenced* vs *delayed,* P = 0.007;

delayed vs *control*, P = 0.62). We also quantified the proportion of place cells which shifted their place fields so that their fields did not overlap between the pre- and post-learning exploration epochs (Figure 3e; online Methods). The majority of *control* and *delayed* silenced neurons preserved their place fields, as only a small fraction of neurons (control group: 85/283, 30%; delayed group: 23/81, 24%) showed non-overlapping place fields. In contrast, a larger fraction of neurons shifted their place preference in the *silenced* group (75/167, 45%; P = 5.8 x 10^{-4}, χ^2 test for 3 groups; *silenced* vs *control*, P = 0.004; *silenced* vs *delayed*, P = 0.04; *delayed* vs *control*, P = 1; two-tailed Fisher's exact test with Bonferroni correction; Supplementary Fig. 8).

In the second approach, which divided place cells by the type of perturbation (ripple-locked/ripple-delayed paradigms), the pixel-by-pixel Pearson correlation between the rate maps obtained from the pre- and post-learning exploration epochs was significantly different between the *ripple-locked* and the *ripple-delayed* groups (n = 385 and n = 247 place cells, respectively; P = 0.007; Mann-Whitney U test; Supplementary Fig. 9h). We found no reliable correlation between the light response indices of individual place cells and their stability, as assessed by the correlation coefficient of their pre- and post-learning rate maps (Supplementary Fig. 9i). This observation suggests that map stability largely depends on the timing of neuronal suppression relative to SPW-Rs (locked versus delayed). However, among the *ripple-locked* place cells, but not among *ripple-delayed* neurons, those that switched their place field preference (no overlapping place fields between pre and post-learning explorations) were more strongly suppressed by light as compared to non-switching place cells (Supplementary Fig. 9k-l). This result indicates that the most strongly suppressed cells in the *ripple-locked* group showed the largest place field shifts. This observation is in line with results from the first approach, which demonstrated that SPW-R-suppressed (*silenced*) place cells had less stable place fields than *control* (non-supressed) ones. Both approaches show that suppressing neuronal activity during SPW-Rs at the goal locations alters the place map of many place cells, with the largest impact on the most strongly suppressed ones. Overall, this result further confirms that activity during SPW-Rs is necessary for stabilizing place fields of pyramidal neurons.

Importantly, differences in place field stability across the *silenced*, *control* and *delayed* groups observed with the first approach could not be explained by mean or peak firing rate differences, since these values did not differ across groups or between the pre- and post-learning epochs (Supplementary Fig. 10b-c). One could also hypothesize that *silenced* neurons would lose their initial place fields and not even be classified as place cells in the post-learning epoch. However, the three groups showed a similar proportion of neurons that lost and gained place fields between the pre- and post-learning exploration epochs (Supplementary Fig. 10e-f). Similarly, *ripple-locked* and *ripple-delayed* neurons defined via the second approach did not differ in terms of firing rates or proportions of place cells (Supplementary Fig. 9b-e). Moreover, place cell remapping was not related to measures of recording instability (Supplementary Fig. 11a-d). These observations indicate that although silenced individual place cells change their spatial representation following SPW-R silencing, they still effectively carry spatial information.

Europe PMC Funders Author Manuscripts

SPW-R-triggered pyramidal cell silencing impairs place map refinement

SPW-R silencing could also impact the amount of spatial information carried by place cells. To explore this possibility, we compared the information content (bits/spikes) carried by each place cell between the pre- and post-learning epochs (Fig. 4a-c). We found that place cells in the *control* group carried more spatial information per spike in the post-learning epoch compared to the pre-learning epoch (Fig. 4a ; P = 0.007, Wilcoxon's paired signed rank test; n = 283). In contrast, information content of *silenced* place cells did not increase significantly from pre-learning to post-learning epoch (Fig. 4c; P = 0.86; n = 167). Related measures of place field features followed a similar trend: sparsity decreased and selectivity increased between the pre- and post-learning epochs in the *control* group (sparsity, P = 0.01; selectivity, P = 0.04) . In contrast, these measures remained unchanged in the *silenced* group (sparsity, P = 0.97; selectivity, P = 0.44). Importantly, the information content carried by place cells was similar across the experimental groups in the pre-learning epoch (i.e., before optogenetic manipulation; Kruskall Wallis test, P = 0.18; 0.74 ± 0.03, 0.70 ± 0.05 and 0.68 ± 0.04 for *control*, *delayed* and *silenced* groups, respectively). Using the second approach, we confirmed that in the *ripple-delayed* (control) group, spatial information per spike increased significantly in the post-learning exploration epoch compared to the pre-learning epoch (P = 0.00007; n = 247; Wilcoxon's paired signed rank test), whereas no difference was detected in the *ripple-locked* group (P = 0.49; n = 385; Supplementary Fig. 9f-g). Overall, these observations suggest that the activity associated with SPW-Rs surrounding reward consumption contributes to the refinement of the cognitive map coded by place cells.

Perturbation of SPW-R-associated activity results in de-stabilized spatial representations of place cell ensembles

In the hippocampus, the representation of each spatial location relies on the coordinated activity of multiple neurons2. We thus tested whether optogenetic SPW-R-triggered pyramidal cell silencing during learning impacts the stability of the spatial representation at the population level, mirroring the effects we saw at the level of individual place cells. The stability of the spatial representation coded by ensembles of place cells was quantified by a population vector analysis30,32 (Fig. 5a-d). For each ensemble of simultaneously recorded place cells (at least 5 place cells in each ensemble; range: 5-28), the median correlation coefficient (computed across across all pixels between the pre- and post-learning exploration epochs) was defined to as a "stability score". This measure provided an estimate of the consistency of the spatial representation at the neuronal ensemble level (n = 24, n = 6, n = 16 ensembles for *control*, *delayed* and *silenced* ensembles, respectively; Supplementary Table 1). Stability scores differed between the three groups (stability scores : 0.68 ± 0.02; 0.72 ± 0.02 and 0.55 ± 0.03 for *control*, *delayed* and *silenced* ensembles, respectively; P = 0.009; Kruskall Wallis test; Fig. 5e): *silenced* assemblies showed a lower stability score than the *control* and *delayed* ensembles (*post-hoc* Tukey's tests; P = 0.01, for *control* vs. *silenced*; P = 0.07 for *delayed* vs. *silenced*; *control* vs. *delayed:* P = 0.94). Using the neuron assignment of the second approach, we also observed a consistent difference between the stability scores of *ripple-delayed* and *ripple-locked* place cell ensembles (P = 0.009; n = 19 *ripple-locked* and 12 *ripple-delayed* ensembles; Mann-Whitney U test; Supplementary Fig. 9m-o).

To control for the possibility that the aforementioned ensemble destabilization effect of SPW-R-triggered silencing was due to inter-session variability in the stability of place cell ensembles, we performed within-session comparisons. On some recording days, we recorded from sufficient numbers of neurons that allowed comparison between *silenced* and *control* or *delayed* and *control* neurons ensembles in the same mouse (n = 15 sessions with *control* and *silenced* ensembles; n = 6 sessions with *control* and *delayed* ensembles; Fig. 6a). In 12 of the 15 *control-silenced* sessions, the stability score was higher in the *control* compared to the simultaneously-recorded *silenced* ensemble (P = 0.02; Wilcoxon's paired signed rank test) (Fig. 6b). In contrast, the *delayed* ensembles showed both higher and lower stability scores than the simultaneously-recorded *control* ensembles, and no group effect was observed (P = 0.84) (Fig. 6b). The stability score differences between the pairs of simultaneously recorded ensembles was larger for *control-silenced* pairs, compared to *control-delayed* pairs (Fig. 6c; P = 0.05; Mann-Whitney U test). Similar results were obtained after controlling for ensemble size (Supplementary Fig. 12, online Methods). These within-session differences between control and manipulated place cell populations present further evidence that activity during awake SPW-R promotes stabilization of place representation coded by hippocampal neuron ensembles.

SPW-R perturbation does not affect place field stability in a cue-guided task

Following the main experiment, mice were trained in a cue-guided task during which the goal locations were signaled by local cues placed next to the three baited wells. In this "cued" version of the task, mice could rely on the cues to find the rewards instead of depending on memorized internal representation of goal locations 30, resulting in a flat learning curve (Supplementary Fig. 13a; n = 10 sessions in 4 mice). Closed-loop SPW-Rs disruption pyramidal cell activity was conducted in those experiments, as for the non-cued version of the task. Place fields were significantly more stable than in the non-cued version of the task and importantly, they were no affected by SPW-Rs optogenetic disruption at the goal locations (Supplementary Figure 13b). This observation suggests that neuronal silencing during SPW-Rs *per se* does not affect the hippocampal map in absence of memory requirements.

Place cell silencing during awake SPW-Rs does not impact their activity during SPW-R of slow wave sleep

In order to test whether our manipulation of awake SPW-Rs had an impact on sleep SPW-Rs, we analyzed the activity of place cells during the SPW-Rs of slow wave sleep, detected during the rest periods in the home cage preceding and following learning. First, we compared the changes in firing rates, participation, spike count and gain between the pre-learning and the post-learning sleep/rest SPW-Rs, across the three groups of place cells (*control*, *delayed* and *silenced*). No differences were found between these groups (Supplementary Fig. 14a), indicating that SPW-Rs suppression of pyramidal neurons during waking does not impact the activity of neurons during sleep SPW-Rs13, at least for the parameters that we considered. Furthermore, we did not detect any reliable relationship between the changes in SPW-R activity (rate, participation, spike count or gain) and place map stability of individual place cells (Supplementary Fig. 14b-e), suggesting that those parameters did not predict the magnitude of remapping of place cells. Yet, our results do not

rule out the possibility that using a considerably larger data set and more sophisticated analyses, place cell silencing may exert an impact of sleep SPW-R content.

Discussion

During exploration, two distinct classes of behaviors alternate: preparatory behaviors, including locomotion of the animal from place to place (foraging), and consummatory behaviors, including transient immobility and food/water consumption33. These two behavioral classes are respectively associated with theta and SPW-R patterns in the hippocampus18,34. One hypothesized role of consummatory states is to maintain the cognitive map26 and prepare the animal to calculate new routes in a familiar environment24,35. SPW-Rs occurred regularly at reward locations when the animal momentarily stopped and drank water. Aborting the buildup of SPW-Rs by optogenetic means at the reward locations reduced place field stability tested across pre-learning and post-learning exploration epochs. This was expressed by the reduced correlation of place fields at both single neuron and population level, place field shifts, impaired spatial information content of spikes and related measures, without any effect on firing rates. Importantly, our selective and focal optogenetic perturbations suppressed spiking in only a small group of pyramidal cells with a minimal effect on neighboring networks and without affecting memory performance. Our findings suggest that the small number of place cells silenced during SPW-Rs were ‘left out’ from the ongoing map stabilization process. Overall, these results support the hypothesis that SPW-Rs promote the maintenance of the cognitive map12,24.

SPW-Rs and stabilization of the hippocampal map

The stability of the cognitive map may deteriorate spontaneously or be modified by various perturbations. Rats re-entering the same environment have been tacitly assumed to have stable spatial maps1,36. However, recent experiments suggest that the cognitive map destabilizes over time32,37. Moreover, firing rates and place field sizes undergo changes during the first few trials, even after repeated exposure to the same familiar environment38. During these early trials the running speed is typically slow, the animal often rears, “scans” the environments39 and stops frequently. SPW-Rs during such immobility periods may be instrumental in maintaining the cognitive map12,24. In our experiments, distal environmental cues and the maze itself remained unchanged from day to day and therefore, in principle, no novel construction of the spatial map was needed. Yet, it is possible that learning and recalling the new goal locations contributed to a de-stabilization of the hippocampal map40, supporting the view that incorporating new information in a pre-existing knowledge41 (or "schema") necessitates a re-consolidation process28. Our experiments showing that control place fields are more stable in the cue-guided task as compared to the non-cued (“memory”) version of the task are in line with this theory (Supplementary Fig. 13). Our observation that optogenetic disruption of place cell activity during awake SPW-Rs at the goal locations affects their spatial representation in the memory version of the task, but not in the cue-guided version of the task, further suggests that SPW-Rs may be involved in the re-consolidation process. The idea that SPW-Rs have a “stabilizing” role in specific conditions of memory requirements is also supported by the

fact that place field remain stable in a well-learned working memory task, despite SPW-Rs disruption13. Complementary to our findings, recent experiments showed that global and extended silencing of CA1 neurons during exploration29, or during SPW-Rs of sleep following exploration of a novel environment, affected place field stability22 (but see23). On the basis of these findings, we hypothesize that neuronal activity during awake SPW-Rs is important for hippocampal map stabilization when new configurations within the map are learned.

Learning performance observed in mice was comparable to that of rats trained in a similar task30. However, in contrast to rats30, we did not observe a goal-related reorganization of place fields (Supplementary Fig. 15). The correlation maps obtained by population vector analysis of SPW-R-silenced place cells did not show any consistent spatial pattern with regards to goal locations or other locations in the maze (Fig. 5 and 6) and the probability of a place cell to fire at goal areas did not predict the magnitude of its place field change (Supplementary Fig. 11e). These observations suggest that SPW-R silencing did not impact the representation of specific regions of the environment. Instead, representation of *any* location of the maze had a similar chance to be affected. We therefore hypothesize that participation in SPW-Rs contribute to the global maintenance of a singular map of the environment.

Mechanisms of SPW-R-assisted maintenance of place map

In novel or changing environments, CA1 and CA3 neurons remap at different rates30,32,42,43. Notably, CA3 place fields are more stable than CA1 place fields across repeated exposures to the same environment30,32,43. Since CA3 constitutes the major drive to CA1 during SPW-Rs4, SPW-Rs may be responsible for restoring a coherent representation between CA3 and CA1 regions.

Alternatively, SPW-Rs may stabilize and refine CA1 place fields through a local impact on CA1 circuits. Indeed, ample evidence suggests the importance of local processing within the CA1 region. Whereas the CA3 drive can contribute to the sequential firing of CA1 neurons during SPW-Rs, CA1 sequences can be also supported by local interactions between pyramidal cells and interneurons44, indicating CA3 input-independent coordination in CA1 circuits. Local inhibition may shape the composition of cell assemblies for specific regions of space3,29 and changes in interneuron networks have been shown to mirror place field re-organization during learning in CA145. These considerations suggest that the place map in CA1 is not simply inherited from upstream regions but local processing contributes importantly to map stability.

Results from the ripple-delayed control group and from the cue-guided version of the task, demonstrate that transient optogenetic hyperpolarization *per se* does not affect CA1 place fields. Indeed, we did not find consistent differences between the non-light-modulated *control* and the *delayed* silenced place cells in any stability measure. Furthermore, optogenetic hyperpolarization during SPW-Rs at goal locations in a control cue-guided task did not affect place field stability (Supplementary Fig. 13b). These control experiments suggest that optogenetic hyperpolarization does not induce a destabilization but rather *prevents* a stabilization process to occur during SPW-Rs in the context of learning. The

plasticity mechanisms associated with SPW-Rs (that would support such stabilization) yet remain to be understood. During SPW-Rs, spiking activity of CA1 neurons coincides with their organized CA3 inputs: dendritic spikes may be induced and somadendritic backpropagation of spikes facilitated46. The coincidence of backpropagating spikes and the EPSCs evoked by the spike-inducing inputs has been shown to induce synaptic plasticity47. Dendritic subthreshold activity during SPW-Rs could also support plasticity in the absence of somatic action potentials48,49. In our study, optogenetic hyperpolarization of pyramidal neurons during SPW-Rs could have impacted these potential plasticity mechanisms preventing the stabilization of the hippocampal map. Reward consumption is not only associated with SPW-Rs in the hippocampus but also with spike bursts in dopaminergic neurons of the ventral tegmental area 50. The reward-induced temporal correlation between enhanced dopaminergic activity and SPW-R-related population bursts in the hippocampus may be critical in the place cell stabilization process.

Overall, our observations suggest that SPW-Rs represent specific time windows during which neurons engage in plasticity mechanisms essential for maintaining and refining the cognitive map. These physiological findings demonstrate why it is beneficial that ambulatory movements are interrupted by consummatory actions during exploration and learning. Furthermore, they provide mechanistic insights into why SPW-R-related activity supports memory function.

Online Methods

Subjects and electrode implantation

All experiments were approved by the Institutional Animal Care and Use Committee of New York University Medical Center. We used transgenic mice to obtain expression of exogenous light-sensitive opsins51: four mice expressed archaerhodopsin-352 (“Arch”) under control of the pyramidal cell selective calcium/calmodulin-dependent protein kinase II alpha - CaMKIIalpha - promoter (referred to as CaMKII-cre::Arch) and one mouse expressed channelrhodopsin-253 (“ChR2”) under the parvalbumin - PV - promoter, primarily expressed in a subpopulation of inhibitory interneurons (referred to as PV-cre::ChR2; Supplementary Fig. 1 and 5, Supplementary Table 1). The inclusion of the PV-cre::ChR2 mouse did not change the overall conclusions drawn from our study (Supplementary Fig. 2). Mice were obtained by breeding the cre-dependent “responder” lines expressing Arch (Ai35D allele; Jackson stock no. 012735) and ChR2 (Ai32 allele; Jackson stock no. 024109) with the “driver” lines expressing the Cre recombinase under the CaMKIIalpha54 (Jackson stock no. 005359) and PV55 (Jackson stock no. 008069) promoters. These five adult male mice (3-5 months old) were implanted unilaterally or bilaterally with high-density silicon probes (32 or 64 sites; Buz32 or Buz64; NeuroNexus), attached to movable microdrives (Fig. 1a), under isoflurane anesthesia, as described previously56. In all experiments, ground and reference screws were implanted in the bone above the cerebellum. Probes were implanted perpendicularly to the midline, or with a 45-degree angle along the hippocampal long axis, at the following coordinates: AP: -1.7 mm; ML: +1 or -1 mm (left or right hemisphere). Two mice were implanted at AP: - 1.8, ML: +/- 1.4. During surgery, the tips of the probes were lowered to the neocortex (depth: 700 μm). After 4–7 d of recovery, they

were moved gradually (≤70 μm/day) until reaching the CA1 pyramidal cell layer of the dorsal hippocampus, characterized by large amplitude ripple oscillations. Neuronal spiking activity and LFP were recorded daily in the behavioral task (Fig. 1a) and the position of the probe was optimized at the end of each daily session to obtain the maximal unit yield. The composition of spiking population varied from session to session due to either active movement of the probe or to spontaneous movement of the brain tissue. We cannot exclude some overlap between the units recorded in the different sessions from the same animal. However, this was not considered as an issue since from day to day, we varied the positions of the rewards on the maze (new learning), and other parameters such as the type of light stimulation (with or without delay), and the identity of the illuminated shanks (for mice with multiple diodes). At the end of the experiment, electrolytic lesions were done by passing current through the bottom sites of the shanks (5μA for 5sec) and mice were perfused 2 days later. Probe shank locations were verified by histology (Supplementary Fig. 1b-c).

Diode-probes

The probes consisted of 4 or 8 shanks (200-μm shank separation) and each shank had 8 recording sites (160 μm^2 each site, 1–3-MΩ impedance), staggered to provide a two-dimensional arrangement (20-μm vertical separation) (Buz32 or Buz64; NeuroNexus). One or more multimode optical fibers (core diameter: 50 μm) were attached to the probe shanks, terminating in a tip etched to a point above electrode sites. At the other end, fibers were coupled to laser diodes56 (450 nm blue laser diode for ChR2 activation; 639 nm red laser diode or 520 nm green laser diode for Arch activation) (Fig. 2a). Both red and green illumination could effectively suppress pyramidal cell spiking in CaMKII-cre::Arch mice. Peak light power, measured at the tip of the shanks before implantation, was: 191±11 μW (mean ± SEM; n = 2 blue laser diodes), 320 ± 73 μW (n = 3 red laser diodes) and 151±19 μW (n = 6 green laser diodes).

Data acquisition

During the recording session, neurophysiological signals were acquired continuously at 20 kHz on a 256-channel Amplipex system (Szeged, Hungary; 14-bit resolution, analog multiplexing)57. The wide-band signal was downsampled to 1.25 kHz and used as the LFP signal. A three-axis accelerometer (ADXL-330, Analog Devices) was attached to the signal multiplexing headstage for monitoring movements. For tracking the position of the mouse on the cheeseboard maze and in its home cage, two small light-emitting diodes, mounted above the headstage, were recorded by a digital video camera at 30 frames/s. The LED locations were detected and recorded online with a custom-made tracking software.

Pre-training

All mice were free from prior manipulation before being included in this study and were maintained on a 12h:12h light-dark cycle (lights on at 07:00 a.m.) in the vivarium (maximum 5 adult mice per cage; housed individually after surgery). Before electrode implantation, the mice were handled daily for at least one week and pre-trained on the spatial learning task on the cheeseboard maze. All experiments were done during the day (light-cycle). Pre-training consisted first in simple exposure to the platform and the start box, 1 hour daily, during two days while water deprivation started. On the two following days, the

mouse was allowed to collect ~20 water rewards (10 μL each) placed in the wells at random locations on the maze. On subsequent days, the animal was trained to locate three water rewards per trial (see below). No probe test was conducted during pre-training. Pre-training was completed when the mouse was able to perform at least 20 trials per session (3 to 4 days). It was then allowed to recover from water deprivation and regain full weight.

Behavioral training

Mice were trained to perform a spatial learning task on a cheeseboard maze, similarly to the task previously described for rats30,58. The maze consisted of a circular platform 80 cm in diameter with 177 wells (1.5 mm deep; 4 mm in diameter; 5 cm spacing between the wells) and a start box placed next to the platform (Fig. 2d). Access to the platform from the start box, and to the start box from the platform, was controlled by a manually operated door. Each daily session consisted of five epochs during which hippocampal activity and behavior were continuously recorded: (1) a pre-learning exploration epoch, (2) a rest epoch, (3) a learning task, (4) a rest epoch and (5) a post-learning exploration epoch (Fig.1a). For the two rest epochs, the animal was returned to its home cage and allowed to sleep for ~1 hour. During these rest epochs, the light in the recording room was on in order to favor sleep, whereas only dim light was used during the learning task and the pre- and post-exploration epochs. The mouse was exposed to the cheeseboard maze during the two exploration epochs and the learning task. During the learning task, mice learned the locations of three hidden water rewards (5 μL) on the cheeseboard maze, out of 177 possible wells (Fig.1c). A new set of three baited wells was randomly selected every day but stayed fixed within a given day. A trial was completed once the mouse had retrieved the three rewards and returned to the start box (median: 50 trials; range: 29 – 60 trials; n = 29 sessions, 5 mice). Access to the start box was conditioned upon successful retrieval of the three baits. However, a trial was aborted and the animal was allowed to return to the start box in the rare cases when the three water rewards were not collected within 4 minutes (from trial start). To prevent the possible use of an odor-guided search strategy that could interfere with spatial learning, the cheeseboard platform was rotated relative to the start box between trials. In addition, the maze was wiped after every 5 trials and at the end of each pre- and post-learning exploration epochs with a tissue paper soaked in alcohol. Thus, goal locations were defined in an extra-maze reference frame. The pre- and post-learning exploration epochs were used to (1) test memory performance and (2) obtain the place fields of the recorded cells for the entire maze. Each epoch was divided into 3 periods (or ‘blocks’) of 10min:

- Block 1: free exploration without any reward
- Block 2: the mouse was presented with a first set of 5 water rewards placed at random locations (same locations for the pre- and post-learning explorations) to encourage exploration of the entire maze
- Block 3: the mouse is presented with a second set of 5 water rewards placed at random locations (same locations for the pre- and post-learning explorations) to encourage exploration

Blocks 2 and 3 are therefore identical (random search) but the rewards are replenished half way. The mouse was allowed to return to the start box between each block. This strategy was

Europe PMC Funders Author Manuscripts

used to promote complete spatial exploration of the platform, a necessary condition to study the spatial information coded by hippocampal assemblies. For quantifying memory performance after learning, only the first (unbaited) block of each pre/post-learning exploration epoch was considered, whereas all three blocks were used for comparing place cell activity. Memory performance was assessed by calculating the proportion of time the mouse spent in the goal areas (15 cm diameter circular regions centered on goal locations) relative to the block duration (10 min) in the pre- and post-learning exploration epochs (Fig. 1d). When comparing learning performance in ripple-delayed and ripple-locked paradigms, only sessions where a single type of paradigm was delivered during learning were considered (i.e., we excluded sessions where both ripple-locked and ripple-delayed stimulations were used in different hemispheres). Learning performance during the learning task was assessed by the distance traveled to retrieve the rewards during each trial or the time it took for the mouse to collect the three rewards (Fig. 1c).

In a subset of sessions (10 sessions in 4 mice), the learning task was modified and the locations of the rewards were signaled by white plastic cylinders, placed next to the baited wells (“cue-guided version” of the task)30. Under these conditions, the animal reaches maximal performance during the first trial and, therefore, the learning curve is flat (Supplementary Fig. 13a). Optogenetic manipulations were conducted as described previously for the non-cued version of the task.

Unit clustering and neuron classification

Spikes were extracted from the high-pass filtered signals (median filter, cutoff frequency: 800 Hz) offline, the waveforms were projected onto a common basis obtained by principal component analysis (PCA) of the data, and sorted into single units automatically using KlustaKwik59 followed by manual adjustment using the software Klusters60 (http://neurosuite.sourceforge.net/). For each unit, the single recording site with the maximal trough amplitude mean waveform was selected and two waveform features were computed: the trough-to-peak and the spike width (the inverse peak frequency of the spike spectrum, estimated by 1024-point FFT of the zero-padded waveforms). This generated two clearly separable clusters (Supplementary Fig. 3a). Putative pyramidal (PYR) and interneurons (INT) were identified based on a Gaussian-mixture model using these two waveform features61. This model was previously built on the waveforms of optogenetically tagged neurons, and neurons showing mono-synaptic connections in the hippocampal CA1 region. It enabled assigning a P-value to the classification of each unit and units with low classification confidence ($p>0.05$) were discarded (21/1406 units, 1.5%). When the identity of a unit defined by this method was considered ambiguous, it was also excluded from the analysis (138/1406 units, 9.8%). Classification of units as PYR and INT was done blindly, i.e., without a priori knowledge of the group the unit belonged to (*control*, *delayed* or *silenced*). We recorded a total of 1406 well-isolated units from CA1 of 5 freely-moving mice in 29 sessions (Supplementary Table 1). Of these, 1020 were putative pyramidal cells and 227 were putative interneurons. 159 well-isolated units were not classified. Stability of our unit recordings across each daily session was checked by comparing the Mahalanobis distance (how well is a given unit isolated from other unit clusters) and the spike waveform

amplitude (on the electrode site with maximal amplitude) in the pre- and the post-exploration epochs (Supplementary Fig. 11a-d).

Optogenetic suppression of pyramidal neurons

The response of each recorded unit to light was tested with a series of light pulses applied during the first rest epoch of each daily recording session (~ 300 pulses per LD, 100 ms each, one pulse every 5 s). This response mapping procedure allowed us to compare the firing rate of each unit before (baseline) and during the light pulses (baseline: 100 ms intervals starting 1 s before each stimulus onset). A unit was considered light-suppressed when the mean firing rates during the light pulses (R_{light}) were significantly reduced as compared to baseline activity ($R_{baseline}$) ($P < 0.05$, Wilcoxon's signed-rank test for matched values, one-tailed test). We computed the light-response index for each unit according to the following formula:

$$\text{Light- response index} = (R_{light} - R_{baseline})/(R_{light} + R_{baseline})$$

An index of value "zero" indicates no change as compared to baseline; "negative one" indicates complete silencing (Supplementary Fig. 3b and 4). In case of bilateral light delivery and recording, only the response to the light stimulus delivered ipsilaterally to the recorded cell was considered. Units classified as *control* included non-significantly modulated neurons (neither suppressed, nor excited during light pulses; $P > 0.05$, Wilcoxon's signed rank tests) recorded exclusively from non-illuminated shanks (Fig. 2f-g). Of the 1020 recorded putative pyramidal cells, 79 were excluded because they were not identified as light-responsive and were located on illuminated shanks (excluded control cells) and 59 were excluded because they showed an increased activity during light pulses. A neuron was also discarded if its baseline firing rate was too low to determine whether a spike count of zero during light pulses was distinct from the spike count expected by chance (20 out of 1020 pyramidal cells). Assuming a Poisson distribution of the neuron spike counts, the minimal (expected) number of spikes during the total light pulse duration (lambda) that could, simply by chance, result in zero spikes is 3 for an alpha level of 0.05. Therefore, with 30 s of response mapping light pulses (300 pulses of 100 ms), cells that fired less than 0.1 spikes/s during baseline were excluded. Of the remaining putative pyramidal cells, 273 units were silenced by SPW-R-triggered light pulses, 129 units were silenced with a delay (100-300 ms following SPW-R detection) and 460 served as control units.

SPW-R-triggered closed-loop light stimulation

A single channel from the middle of the CA1 pyramidal cell layer with the largest amplitude ripple was selected for real-time processing of LFP by a programmable digital signal processor (DSP) running at 25 kHz (RX6, Tucker-Davis Technologies). The root-mean-square (RMS) of the band-pass filtered (80-250 Hz) signal was computed in two running windows, long (2 s; RMS1) and short (8 ms; RMS2). Ripples were defined as events with RMS2 exceeding three times RMS1 (range: 3-3.5) for at least 8 ms31. Light stimuli (60 ms square pulses, one pulse per detection) were applied in a closed-loop manner during the learning task, exclusively when the mouse was located at the reward locations (15 cm

Europe PMC Funders Author Manuscripts

diameter circular areas centered on the three baited wells) (“ripple-locked” paradigm) (Fig. 2d). This spatially-conditioned stimulation was achieved using a custom tracking software which detected, in real time, the periods when the mouse was located within the pre-defined goal areas. As a control, delayed stimuli (60 ms pulses, one pulse per detection) were presented at random intervals between 100 and 300 ms following SPW-R detection (“ripple-delayed” paradigm). Ripple-delayed and ripple-locked paradigms were presented in a pseudo-randomized manner in the same animal subjects, either on different recording sessions, or in combination but in different hemispheres (see Supplementary Table 1).

In order to quantify the effectiveness of the online SPW-R detection, we used the first 3 min of the post-learning epoch when the online detection was conducted but no light stimulus was delivered. During this period, the mouse was in the start box before being released for exploration. SPW-Rs that occurred during immobility periods (< 3cm/s movement) were visually identified in each session blindly (without the knowledge of online detection) and subsequently compared to the online detections. Overall, 83 ± 4% of the visually identified SPW-Rs were detected by the online detection program (n = 17 sessions). The SPW-Rs missed by online detection were typically of smaller amplitude events and shorter in duration as compared to online-detected SPW-Rs. Conversely, 63 ± 4% of all online detected SPW-Rs were considered as ‘false positive’ events by the visual scoring. These false positive events were typically due to muscle artifacts or large power fast gamma events during small movements. These falsely detected SPW-Rs necessitated the inclusion of delayed-stimulation control experiments.

Offline detection of SPW-Rs was performed as previously reported31 in order to estimate awake SPW-Rs duration and the delay between online SPW-R detection and SPW-R onset (Supplementary Fig. 6; post-exploration epoch or learning task epoch with delayed paradigms only) and to characterize changes in sleep SPW-Rs activity during slow wave sleep (Supplementary Fig. 14). Briefly, the wide-band signal was band-pass filtered (80–250 Hz; difference-of-Gaussians, DOG; zero-lag, linear phase FIR), and instantaneous power was computed. The mean and SD were computed from the power of the signal during slow wave sleep in the absence of light stimulation. Subsequently, the power of the original trace was computed, and all events exceeding 2.5 SD from the mean were selected. Short events (duration <15 ms) were discarded, and adjacent events (gap <15 ms) were merged. Events were then expanded until the power fell below 2 SD to define event edges. Slow wave sleep periods were defined using hippocampal LFP (theta/delta ratio), accelerometer (movement), as previously described62.

Spatial tuning of place cell activity

Data recorded on the cheeseboard maze were used for the analysis of spatial tuning of spiking activity. Only data during epochs when the mouse was running faster than 5 cm/s were used. Position of the animal was determined by recording LEDs on the head stage at 30 Hz using a custom-made tracking software. The position and spiking data were sorted into 3 cm × 3 cm bins to generate raw maps of spike counts and occupancy. A Gaussian kernel (s.d. = 5 cm) was applied for both raw maps of spike and occupancy, and a smoothed rate map was constructed by dividing the smoothed spike map by the smoothed occupancy map.

The smoothed rate maps obtained for the pre-learning and post-learning exploration epochs were used to compute the mean and peak firing rates in the maze as well as the number of place fields. A place field was defined as a contiguous region of at least 72 cm^2 (eight bins) where the firing rate was above 60% of the peak rate in the maze, containing at least one bin above 80% of the peak rate in the maze63. *Sparsity*, *spatial selectivity*, and *spatial information*64 were computed from the smoothed rate maps63,65. Units with a peak firing rate lower than 0.4 Hz and an information content lower than 0.25 bit/spike were not considered as place cells. If the information content of the cell was similar ($P > 0.05$) to chance level (computed by parsing the spike train of the cell and the position of the mouse – speed > 5 cm/s - into 30s blocks and shuffling these “spikes” and “position” blocks 100 x relative to each other’s65), the cell was also not a considered as place cell. Only putative pyramidal cells that were defined as place cells in the cheeseboard maze (start box excluded) in at least one of the two exploration epochs (pre- or post-learning) were considered for analyses. Of the 1020 putative pyramidal cells 637 were classified as place cells in the maze: 167 were silenced by SPW-R-triggered light pulses (referred to as "silenced"), 81 were silenced with a delay after SPW-R detection (referred to as "delayed") and 283 were control place cells (referred to as "control"). Of the 106 remaining place cells, 15 were discarded because they had undefinable responses due to low firing rates, 52 because they were non-responsive and located on illuminated shanks and 39 because they showed an increase in activity during the light pulses (see “Optogenetic suppression of pyramidal neurons” section).

Statistical analyses

All statistical analyses were performed in Matlab (MathWorks). Number of animals and number of recorded cells were similar to those generally employed in previous reports12–14,25,29,30,38,39,66. All tests were two-tailed unless indicated. For all tests, non-parametric Mann-Whitney U test, Wilcoxon's paired signed rank test and Kruskal Wallis one-way analysis of variance were used. Tukey’s *post-hoc* tests were performed for multiple comparisons. Analysis of place cells properties (remapping, place field characteristics) was done blindly relative to the cell categories these cells belonged to (control, delayed and silenced groups - approach 1 - or ripple-locked or ripple-delayed groups -approach 2-). Outlier values not represented in Figure 4 and S8f-g were included in statistical analysis (their exclusion does not affect the conclusions). Results are displayed as mean ± SEM unless indicated otherwise. When box plots are used (e.g. in Fig. 2c and 2g), on each box, the central mark indicates the median, and the bottom and top edges of the box indicate the 25th and 75th percentiles, respectively. The whiskers extend to the most extreme data points not considered outliers, and the outliers are plotted individually using the '+' symbol.

Quantification of spatial map stability

Place map stability for individual place cells was defined by the bin-by-bin Pearson's correlation coefficient between the firing rate maps of the pre- and post-learning exploration epochs. Only spatial bins visited by the mouse for at least 100 ms during both epochs were taken into account.

Place field overlap—Spatial bins of place fields were defined as described above. The figure below describes the method used to calculate the percentage of overlap between pre- and post-exploration place fields. It represents the area covered by the intersection between the 'pre' and 'post' place fields (red area in Method Figure 1a and 1c) divided by the area covered by their sum. A place cell was considered to have no-overlapping place fields if it displayed 'pre' and 'post' place fields that had no spatial bins in common (Method Figure 1b). Place cells that had place fields in one of the probe session but no place fields in the other probe session were also considered as having non-overlapping place fields. Using less restrictive criteria for place field definition did not affect our observations (Supplementary Fig. 8).

Population vector analysis—Among all recording sessions, we identified sessions with at least 5 place cells ('ensembles') in a given category (*silenced*, *control* or *delayed*) (range: 5 to 28 place cells). For each ensemble, we computed the correlation value obtained for individual spatial bins between the pre-learning and post-learning exploration epochs30,66. The stability score corresponded to the median of these per-bin correlation values obtained for a given ensemble of place cells. Only bins visited by the animal longer than 100 ms during both pre-learning and post-learning exploration epochs were included in this analysis. For the comparison of pairs of simultaneously recorded ensembles (Fig. 6), we used a down-sampling approach in order to control for ensemble size. First, the number of place cells part of the smaller ensemble of the pair (N) was determined. Next, we randomly selected N cells from the larger ensemble of the pair and computed the corresponding stability score as previously described. We repeated this procedure up to 100 times and computed the average stability score obtained from the scores of down-sampled ensembles. This averaged stability score was assigned to the larger ensemble of the pair (see Supplementary Fig. 12).

Goal location representation

Probability of spiking in goal areas—For each neuron, we first computed a "probability map" which indicates the probability of the neuron to emit an action potential in a spatial bin of the maze per time unit. This map was obtained by dividing the rate map of the neuron by the sum of the rates accumulated over all visited spatial bins. From this probability map, we then added the probability values corresponding to the visited spatial bins surrounding the three goal locations (circular areas of 5 cm radius centered on the goal wells). The resulting value was then normalized by dividing it by the total number of spatial bins included in the sum. This procedure was done independently for the pre-learning and the post-learning exploration epochs (see Supplementary Fig. 15a).

Distance of place field to goal areas—Place fields were defined as described previously. For each place field, the shortest distance between its (i) edge, (ii) peak or (iii) centroid and any of the three goal locations was determined. If a neuron had multiple place fields, only the minimal value was considered (ie the place field closest to any goal location) (see Supplementary Fig. 15b).

Histological processing

Mice were anesthetized with pentobarbital (100 mg/kg intraperitoneal) and perfused with saline and 4% paraformaldehyde before their brains were rapidly removed. Coronal sections (100μm) were cut on a vibratome (Leica, VT1000S) and collected in phosphate buffered saline (PBS).

DAPI staining—After 3 washes in PBS (10 min each), sections were permeabilized in PBS containing 0.2% Triton-X100 (PBS*) for 20 minutes. Sections were then incubated for 20 min in PBS* containing DAPI (1:10000; D1306, Molecular Probes), and washed again 3 times (10 minutes each) in PBS. Sections were mounted in Fluoromount (Sigma) and imaged with a wide-field fluorescence microscope (Zeiss, Axioscope).

Parvalbumin (PV) immunostaining—After 3 washes in PBS (10 min each), sections were permeabilized in PBS containing 1.5% of goat serum and 0.2% Triton-X100 (PBS*) for 1 hour and processed for immunostaining by overnight incubation at 4ºC with polyclonal antibodies anti-PV diluted in PBS* (1:500; PV 27, Swant, https://www.swant.com/pdfs/Rabbit_anti_parvalbumin_PV27.pdf). After 2 washes (30min each) in PBS, sections were incubated for 2 hours at room temperature with secondary antibodies (goat anti-rabbit IgGs conjugated with Alexa Fluor 555 dyes; 1:3000; Molecular Probes). After 3 washed (20 minutes each), sections were mounted in Fluoromount (Sigma) and imaged with a confocal laser-scanning microscope.

Data availability

The data that support the findings of this study will be publicly available on the CRCNS.org server after publication.

Code availability

Most of the code used was adapted from the FMAToolbox (http://fmatoolbox.sourceforge.net/). Moreover, the code used in this study is available from corresponding author upon request.

Supplementary Material

Refer to Web version on PubMed Central for supplementary material.

Acknowledgments

We thank N. Chenouard, G. Girardeau, L. Sjulson, A. Peyrache and all members of the lab for invaluable discussions, advice and comments on the manuscript. This work was supported by NIH grants MH107396, MH54671, U01NS090583, the Simons Foundation and the G. Harold and Leila Y. Mathers Foundation. L.R. was supported by the NIH grant K99NS094735 and the Bettencourt Schueller Foundation. E.S. was supported by the Rothschild Foundation, Human Frontiers in Science Program LT-000346/2009-L, Machiah Foundation 20090098, and ERC-2015-StG 679253. B.H. was supported by the National Natural Science Foundation of China (grant no. 31471050).

References

1. O'Keefe, J., Nadel, L. Book The Hippocampus as a Cognitive Map. Oxford University Press; 1978.

2. Wilson MA, McNaughton BL. Dynamics of the hippocampal ensemble code for space. Science. 1993; 261:1055–1058. [PubMed: 8351520]
3. Trouche S, Perestenko PV, van de Ven GM, Bratley CT, McNamara CG, et al. Recoding a cocaine-place memory engram to a neutral engram in the hippocampus. Nat Neurosci. 2016; 19:564–567. [PubMed: 26900924]
4. Buzsaki G, Leung LW, Vanderwolf CH. Cellular bases of hippocampal EEG in the behaving rat. Brain Res. 1983; 287:139–171. [PubMed: 6357356]
5. Wilson MA, McNaughton BL. Reactivation of hippocampal ensemble memories during sleep. Science. 1994; 265:676–679. [PubMed: 8036517]
6. Kudrimoti HS, Barnes CA, McNaughton BL. Reactivation of hippocampal cell assemblies: effects of behavioral state, experience, and EEG dynamics. J Neurosci. 1999; 19:4090–4101. [PubMed: 10234037]
7. Nadasdy Z, Hirase H, Czurko A, Csicsvari J, Buzsaki G. Replay and time compression of recurring spike sequences in the hippocampus. J Neurosci. 1999; 19:9497–9507. [PubMed: 10531452]
8. Lee AK, Wilson MA. Memory of sequential experience in the hippocampus during slow wave sleep. Neuron. 2002; 36:1183–1194. [PubMed: 12495631]
9. Foster DJ, Wilson MA. Reverse replay of behavioural sequences in hippocampal place cells during the awake state. Nature. 2006; 440:680–683. [PubMed: 16474382]
10. Csicsvari J, O'Neill J, Allen K, Senior T. Place-selective firing contributes to the reverse-order reactivation of CA1 pyramidal cells during sharp waves in open-field exploration. Eur J Neurosci. 2007; 26:704–716. [PubMed: 17651429]
11. Diba K, Buzsaki G. Forward and reverse hippocampal place-cell sequences during ripples. Nat Neurosci. 2007; 10:1241–1242. [PubMed: 17828259]
12. Gupta AS, van der Meer MA, Touretzky DS, Redish AD. Hippocampal replay is not a simple function of experience. Neuron. 2010; 65:695–705. [PubMed: 20223204]
13. Jadhav SP, Kemere C, German PW, Frank LM. Awake hippocampal sharp-wave ripples support spatial memory. Science. 2012; 336:1454–1458. [PubMed: 22555434]
14. Pfeiffer BE, Foster DJ. Hippocampal place-cell sequences depict future paths to remembered goals. Nature. 2013; 497:74–79. [PubMed: 23594744]
15. Singer AC, Carr MF, Karlsson MP, Frank LM. Hippocampal SWR activity predicts correct decisions during the initial learning of an alternation task. Neuron. 2013; 77:1163–1173. [PubMed: 23522050]
16. Papale AE, Zielinski MC, Frank LM, Jadhav SP, Redish AD. Interplay between Hippocampal Sharp-Wave-Ripple Events and Vicarious Trial and Error Behaviors in Decision Making. Neuron. 2016; 92:975–982. [PubMed: 27866796]
17. Buzsaki G. Two-stage model of memory trace formation: a role for “noisy” brain states. Neuroscience. 1989; 31:551–570. [PubMed: 2687720]
18. Buzsaki G. Hippocampal sharp wave-ripple: A cognitive biomarker for episodic memory and planning. Hippocampus. 2015; 25:1073–1188. [PubMed: 26135716]
19. Sutherland GR, McNaughton B. Memory trace reactivation in hippocampal and neocortical neuronal ensembles. Curr Opin Neurobiol. 2000; 10:180–186. [PubMed: 10753801]
20. Girardeau G, Benchenane K, Wiener SI, Buzsaki G, Zugaro MB. Selective suppression of hippocampal ripples impairs spatial memory. Nat Neurosci. 2009; 12:1222–1223. [PubMed: 19749750]
21. Ego-Stengel V, Wilson MA. Disruption of ripple-associated hippocampal activity during rest impairs spatial learning in the rat. Hippocampus. 2010; 20:1–10. [PubMed: 19816984]
22. van de Ven GM, Trouche S, McNamara CG, Allen K, Dupret D. Hippocampal Offline Reactivation Consolidates Recently Formed Cell Assembly Patterns during Sharp Wave-Ripples. Neuron. 2016; 92:968–974. [PubMed: 27840002]
23. Kovacs KA, O'Neill J, Schoenenberger P, Penttonen M, Ranguel Guerrero DK, et al. Optogenetically Blocking Sharp Wave Ripple Events in Sleep Does Not Interfere with the Formation of Stable Spatial Representation in the CA1 Area of the Hippocampus. PLoS One. 2016; 11:e0164675. [PubMed: 27760158]

24. Samsonovich AV, Ascoli GA. A simple neural network model of the hippocampus suggesting its pathfinding role in episodic memory retrieval. Learn Mem. 2005; 12:193–208. [PubMed: 15774943]
25. Cheng S, Frank LM. New experiences enhance coordinated neural activity in the hippocampus. Neuron. 2008; 57:303–313. [PubMed: 18215626]
26. Tolman EC. Cognitive maps in rats and men. Psychol Rev. 1948; 55:189–208. [PubMed: 18870876]
27. Nader K, Schafe GE, LeDoux JE. The labile nature of consolidation theory. Nat Rev Neurosci. 2000; 1:216–219. [PubMed: 11257912]
28. McKenzie S, Eichenbaum H. Consolidation and reconsolidation: two lives of memories? Neuron. 2011; 71:224–233. [PubMed: 21791282]
29. Schoenenberger P, O'Neill J, Csicsvari J. Activity-dependent plasticity of hippocampal place maps. Nat Commun. 2016; 7:11824. [PubMed: 27282121]
30. Dupret D, O'Neill J, Pleydell-Bouverie B, Csicsvari J. The reorganization and reactivation of hippocampal maps predict spatial memory performance. Nat Neurosci. 2010; 13:995–1002. [PubMed: 20639874]
31. Stark E, Roux L, Eichler R, Senzai Y, Royer S, et al. Pyramidal cell-interneuron interactions underlie hippocampal ripple oscillations. Neuron. 2014; 83:467–480. [PubMed: 25033186]
32. Mankin EA, Sparks FT, Slayyeh B, Sutherland RJ, Leutgeb S, et al. Neuronal code for extended time in the hippocampus. Proc Natl Acad Sci U S A. 2012; 109:19462–19467. [PubMed: 23132944]
33. Woodworth, R. Book Dynamic Psychology. Columbia University Press; 1918.
34. Vanderwolf CH. Hippocampal electrical activity and voluntary movement in the rat. Electroencephalogr Clin Neurophysiol. 1969; 26:407–418. [PubMed: 4183562]
35. Muller RU, Stead M, Pach J. The hippocampus as a cognitive graph. J Gen Physiol. 1996; 107:663–694. [PubMed: 8783070]
36. Muller RU, Kubie JL. The effects of changes in the environment on the spatial firing of hippocampal complex-spike cells. J Neurosci. 1987; 7:1951–1968. [PubMed: 3612226]
37. Ziv Y, Burns LD, Cocker ED, Hamel EO, Ghosh KK, et al. Long-term dynamics of CA1 hippocampal place codes. Nat Neurosci. 2013; 16:264–266. [PubMed: 23396101]
38. Mehta MR, Barnes CA, McNaughton BL. Experience-dependent, asymmetric expansion of hippocampal place fields. Proc Natl Acad Sci U S A. 1997; 94:8918–8921. [PubMed: 9238078]
39. Monaco JD, Rao G, Roth ED, Knierim JJ. Attentive scanning behavior drives one-trial potentiation of hippocampal place fields. Nat Neurosci. 2014; 17:725–731. [PubMed: 24686786]
40. Kentros CG, Agnihotri NT, Streater S, Hawkins RD, Kandel ER. Increased attention to spatial context increases both place field stability and spatial memory. Neuron. 2004; 42:283–295. [PubMed: 15091343]
41. Tse D, Langston RF, Kakeyama M, Bethus I, Spooner PA, et al. Schemas and memory consolidation. Science. 2007; 316:76–82. [PubMed: 17412951]
42. Lee I, Yoganarasimha D, Rao G, Knierim JJ. Comparison of population coherence of place cells in hippocampal subfields CA1 and CA3. Nature. 2004; 430:456–459. [PubMed: 15229614]
43. Kemere C, Carr MF, Karlsson MP, Frank LM. Rapid and continuous modulation of hippocampal network state during exploration of new places. PLoS One. 2013; 8:e73114. [PubMed: 24023818]
44. Stark E, Roux L, Eichler R, Buzsaki G. Local generation of multineuronal spike sequences in the hippocampal CA1 region. Proc Natl Acad Sci U S A. 2015; 112:10521–10526. [PubMed: 26240336]
45. Dupret D, O'Neill J, Csicsvari J. Dynamic reconfiguration of hippocampal interneuron circuits during spatial learning. Neuron. 2013; 78:166–180. [PubMed: 23523593]
46. Kamondi A, Acsady L, Buzsaki G. Dendritic spikes are enhanced by cooperative network activity in the intact hippocampus. J Neurosci. 1998; 18:3919–3928. [PubMed: 9570819]
47. Magee J, Hoffman D, Colbert C, Johnston D. Electrical and calcium signaling in dendrites of hippocampal pyramidal neurons. Annu Rev Physiol. 1998; 60:327–346. [PubMed: 9558467]

48. Golding NL, Staff NP, Spruston N. Dendritic spikes as a mechanism for cooperative long-term potentiation. Nature. 2002; 418:326–331. [PubMed: 12124625]
49. Bittner KC, Grienberger C, Vaidya SP, Milstein AD, Macklin JJ, et al. Conjunctive input processing drives feature selectivity in hippocampal CA1 neurons. Nat Neurosci. 2015; 18:1133–1142. [PubMed: 26167906]
50. Gomperts SN, Kloosterman F, Wilson MA. VTA neurons coordinate with the hippocampal reactivation of spatial experience. Elife. 2015; 4
51. Madisen L, Mao T, Koch H, Zhuo JM, Berenyi A, et al. A toolbox of Cre-dependent optogenetic transgenic mice for light-induced activation and silencing. Nat Neurosci. 2012; 15:793–802. [PubMed: 22446880]
52. Chow BY, Han X, Dobry AS, Qian X, Chuong AS, et al. High-performance genetically targetable optical neural silencing by light-driven proton pumps. Nature. 2010; 463:98–102. [PubMed: 20054397]
53. Boyden ES, Zhang F, Bamberg E, Nagel G, Deisseroth K. Millisecond-timescale, genetically targeted optical control of neural activity. Nat Neurosci. 2005; 8:1263–1268. [PubMed: 16116447]
54. Tsien JZ, Chen DF, Gerber D, Tom C, Mercer EH, et al. Subregion- and cell type-restricted gene knockout in mouse brain. Cell. 1996; 87:1317–1326. [PubMed: 8980237]
55. Hippenmeyer S, Vrieseling E, Sigrist M, Portmann T, Laengle C, et al. A developmental switch in the response of DRG neurons to ETS transcription factor signaling. PLoS Biol. 2005; 3:e159. [PubMed: 15836427]
56. Stark E, Koos T, Buzsaki G. Diode probes for spatiotemporal optical control of multiple neurons in freely moving animals. J Neurophysiol. 2012; 108:349–363. [PubMed: 22496529]
57. Berenyi A, Somogyvari Z, Nagy AJ, Roux L, Long JD, et al. Large-scale, high-density (up to 512 channels) recording of local circuits in behaving animals. J Neurophysiol. 2014; 111:1132–1149. [PubMed: 24353300]
58. Kesner RP, Farnsworth G, Kametani H. Role of parietal cortex and hippocampus in representing spatial information. Cereb Cortex. 1991; 1:367–373. [PubMed: 1822746]
59. Harris KD, Henze DA, Csicsvari J, Hirase H, Buzsaki G. Accuracy of tetrode spike separation as determined by simultaneous intracellular and extracellular measurements. J Neurophysiol. 2000; 84:401–414. [PubMed: 10899214]
60. Hazan L, Zugaro M, Buzsaki G. Klusters, NeuroScope, NDManager: a free software suite for neurophysiological data processing and visualization. J Neurosci Methods. 2006; 155:207–216. [PubMed: 16580733]
61. Stark E, Eichler R, Roux L, Fujisawa S, Rotstein HG, et al. Inhibition-induced theta resonance in cortical circuits. Neuron. 2013; 80:1263–1276. [PubMed: 24314731]
62. Grosmark AD, Mizuseki K, Pastalkova E, Diba K, Buzsaki G. REM sleep reorganizes hippocampal excitability. Neuron. 2012; 75:1001–1007. [PubMed: 22998869]
63. Mizuseki K, Royer S, Diba K, Buzsaki G. Activity dynamics and behavioral correlates of CA3 and CA1 hippocampal pyramidal neurons. Hippocampus. 2012; 22:1659–1680. [PubMed: 22367959]
64. Skaggs, WE., McNaughton, BL., G, KM., M, EJ. Advances in Neural Information Processing Systems. Hanson, SJ.Cowan, JD., Giles, CL., editors. Vol. 5. Morgan Kaufmann; 1993. p. 1030-1037.
65. Markus EJ, Barnes CA, McNaughton BL, Gladden VL, Skaggs WE. Spatial information content and reliability of hippocampal CA1 neurons: effects of visual input. Hippocampus. 1994; 4:410–421. [PubMed: 7874233]
66. Leutgeb JK, Leutgeb S, Treves A, Meyer R, Barnes CA, et al. Progressive transformation of hippocampal neuronal representations in “morphed” environments. Neuron. 2005; 48:345–358. [PubMed: 16242413]

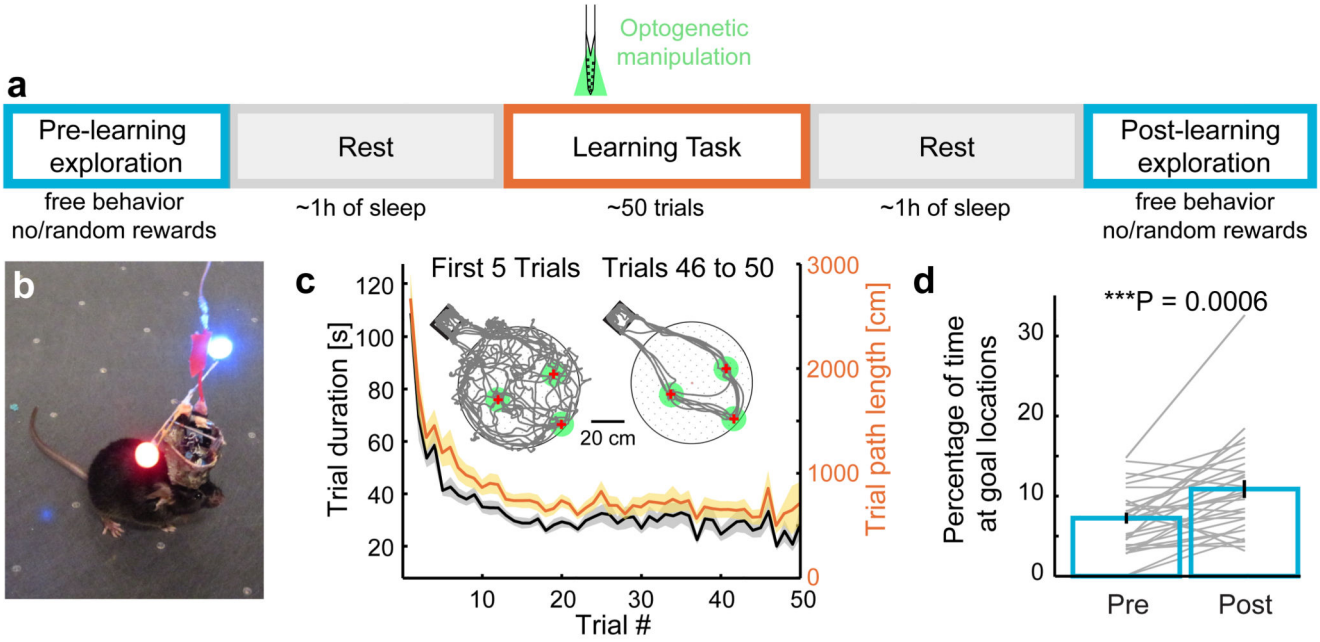

Figure 1. Daily spatial learning of hidden reward locations on the cheeseboard maze.

(a) Five steps constituting a daily recording session30: (1) pre-learning exploration epoch, (2) rest epoch in home cage, (3) learning task, (4) rest epoch in home cage and (5) post-learning exploration epoch. Optogenetic manipulations were conducted during the learning task. **(b)** Implanted mouse equipped with blue and red LEDs allowing real-time position tracking. **(c)** Learning performance during the task. A new set of three baited wells was randomly selected every day but stayed fixed within a given day. Lines with shaded areas show mean ± SEM for n = 29 sessions in 5 mice. **(d)** Mice spent consistently more time at the goal locations during the first 10 min of the post-learning exploration epoch, compared to the first 10 min of the pre-learning exploration epoch (7.2 ± 0.7 and 10.8 ± 1.1 % of the time for pre and post, respectively; ***P = 0.0006, Wilcoxon's paired signed rank test, n = 29 sessions in 5 mice).

Europe PMC Funders Author Manuscripts

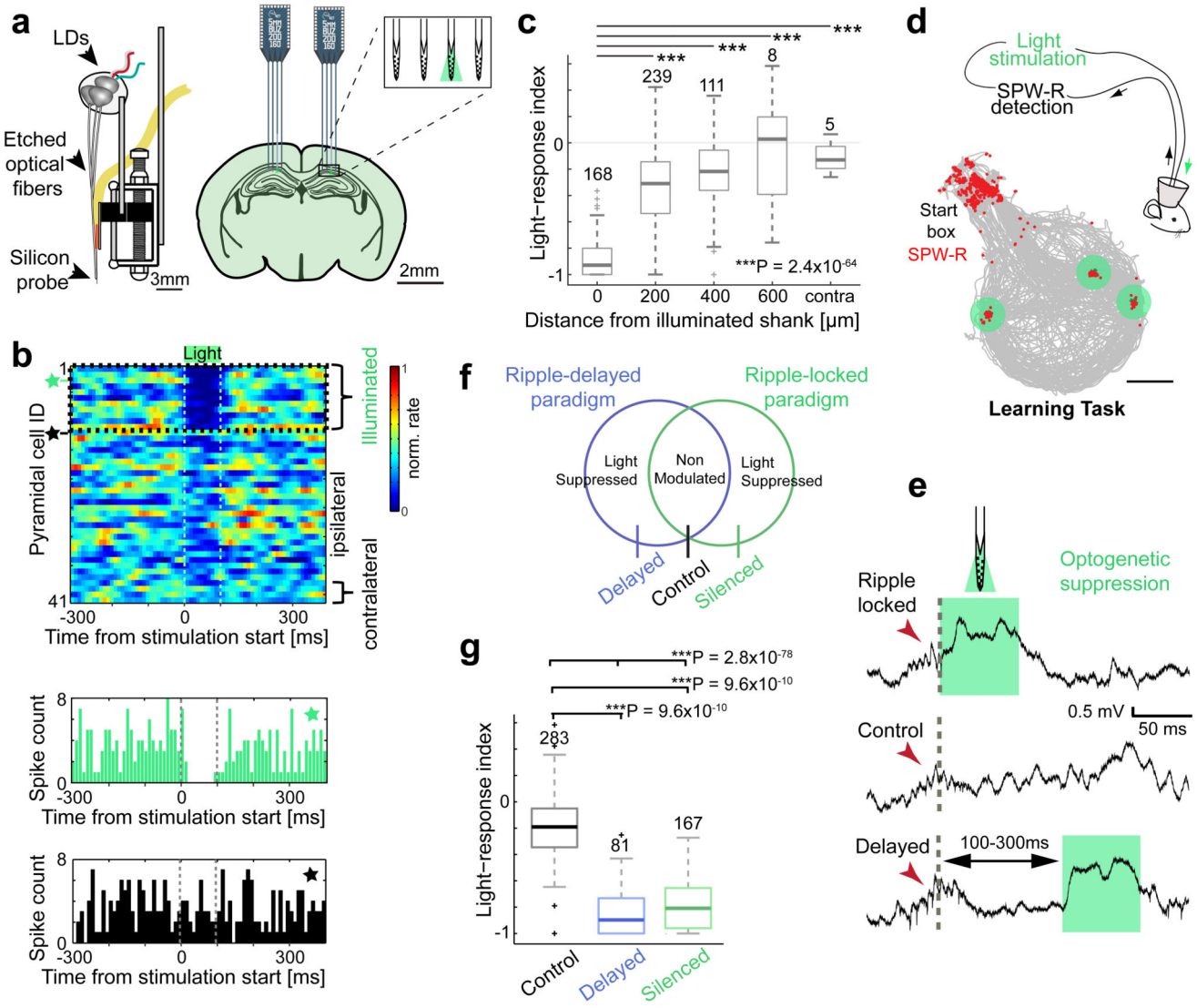

Figure 2. Closed-loop focal optogenetic silencing of pyramidal cells contingent upon SPW-R detection at goal locations.

(a) Left: Schematic of a diode-probe mounted on a movable drive. Right: Diode-probes were implanted uni- or bilaterally in the dorsal CA1 hippocampal region. **(b)** Peristimulus histogram (PSTH) for a population of simultaneously recorded pyramidal cells, illustrating the local silencing effect provided by focal light delivery: units recorded on the illuminated shank (top; black dotted line box) are strongly suppressed during illumination. Below are shown examples of PSTHs for a light-suppressed (green star in top panel) and a control (black star in top panel) pyramidal cell. **(c)** Light response indices as a function of distance from illuminated shank. The number of place cells recorded at each distance is shown above boxes. Indices: -0.88 ± 0.01 (0 µm), -0.34 ± 0.02 (200 µm); -0.24 ± 0.02 (400 µm); -0.06 ± 0.15 (600 µm); -0.11 ± 0.05 (contralateral hemisphere). Kruskall Wallis test: ***P = 2.4 x 10^{-64}; Tukey's *post-hoc* tests: neurons from illuminated shank versus 200 µm neurons, ***P = 9.91 x 10^{-9}; versus 400 µm neurons, ***P = 9.91 x 10^{-9} ; versus 600 µm neurons, ***P =

Europe PMC Funders Author Manuscripts

Europe PMC Funders Author Manuscripts

1.05 x 10^{-7} ; versus contralateral neurons, ***P = 2.00 x 10^{-5}; P > 0.05 for all other comparisons; n = 531 place cells. **(d)** Offline detected SPW-Rs (red dots) are displayed on top of the animal trajectory (gray) for an example learning session. Note that SPW-Rs mainly occur at the goal locations (green disks) and in the start box. 86 ± 2% of all SPW-Rs occurred in the start box (where the mouse stayed mostly immobile) (n = 7 sessions). Light stimuli (60ms) were only triggered by SPW-Rs in the goal areas (green disks). **(e)** Light stimuli aborted ripples locally (top) but had no effect in the control (non-illuminated shank, middle) and delayed (bottom) condition. The positive deflections in the extracellular signal during light stimuli reflect physiological neuronal hyperpolarization44. **(f)** Schematic illustrating place cell classification into three categories based on experimental paradigm (optogenetic stimulation triggered with or without delay relative to SPW-R detection) and their firing rate modulation by light (see online Methods). **(g)** Optogenetic silencing effect in the three groups of place cells. Indices: -0.20 ± 0.01 (*control*), -0.84 ± 0.02 (*delayed*); -0.78 ± 0.02 (*silenced*). Kruskall Wallis test: ***P = 2.6 x 10^{-78}. Tukey's *post-hoc* tests: *control* versus *delayed,* P = 0.52; *control* versus *silenced,* ***P = 9.56 x 10^{-10}; *delayed* versus *silenced,* ***P = 9.56 x 10^{-10}; n = 283, 81,167 *control*, *delayed* and *silenced* place cells.

Europe PMC Funders Author Manuscripts

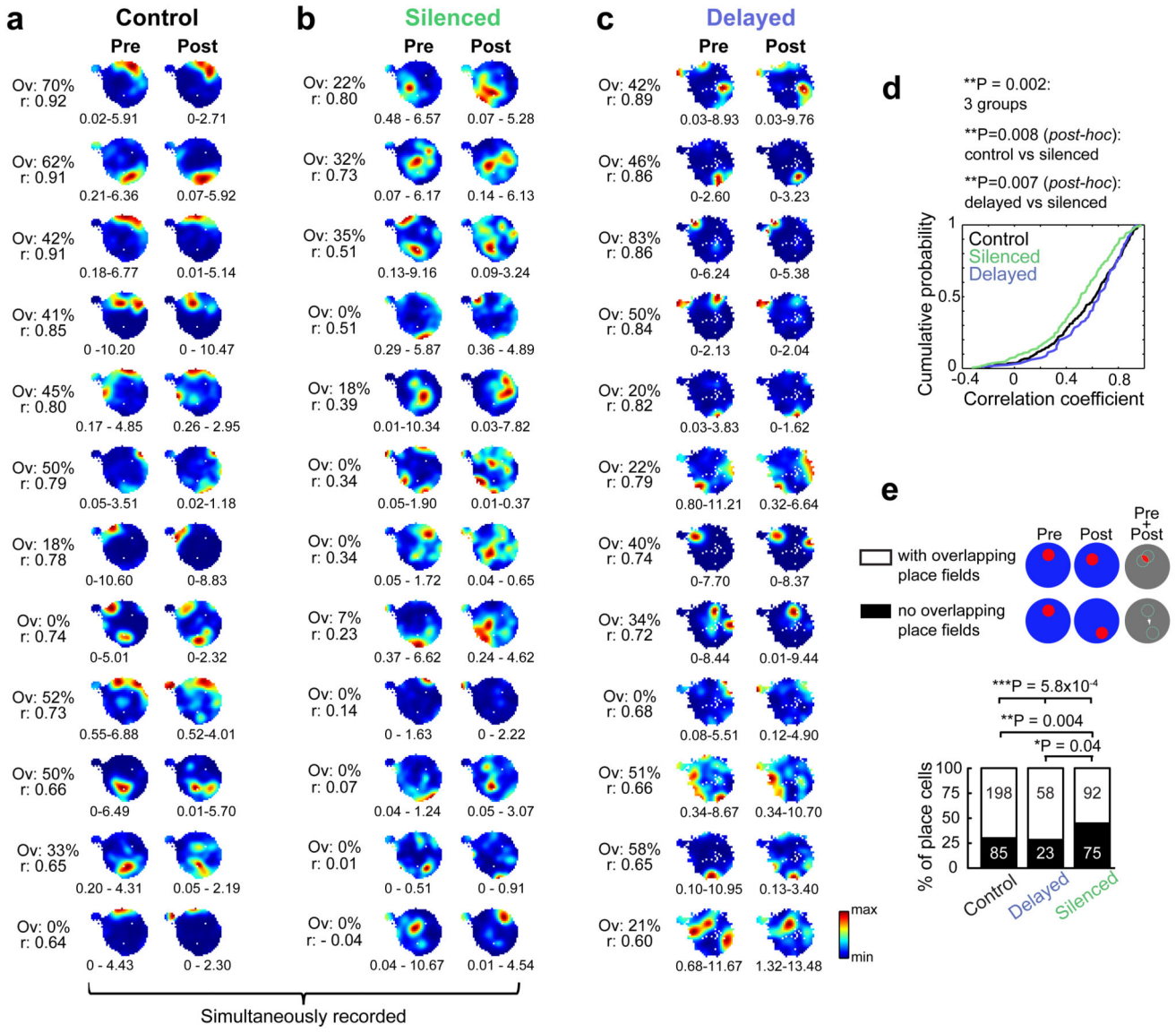

Figure 3. Silencing neurons during SPW-Rs impairs place map stability of place cells.

(a-c) Examples of firing rate maps obtained from the pre- and post-learning exploration epochs in example sessions for individual *control* (**a**), *silenced* (**b**) and *delayed* (**c**) place cells. The correlation coefficient (r), calculated by comparing firing rate maps in pre and post-learning exploration epochs, and the percentage of overlap (Ov) between the place fields detected in these two epochs, is shown for each place cell on the left. 0% overlap indicates shifting place fields ("no overlapping place fields" in **e**). Twelve place cells with the highest r values in each category are depicted. Control and silenced place cells (a and b) were recorded during the same session. **(d)** Cumulative distributions of the r values obtained for individual place cells in the three groups. Kruskall Wallis test: **P = 0.002; Tukey's *post-hoc* tests: **P = 0.008 (control *vs* silenced), **P = 0.007 (delayed *vs* silenced), P = 0.62 (control *vs* delayed); n = 283 control, n = 81 delayed and n = 167 SPW-R silenced place cells. **(e)** Proportions of place cells with shifting fields (no overlapping place fields,

black) or overlapping place fields (white) in the three groups of place cells. The number of cells in each category is indicated on the bars. χ^2 test: ***P = 5.8 x 10^{-4}; *post-hoc* two-sided Fisher's exact tests followed by Bonferroni correction: **P = 0.004 (*control vs silenced*), *P = 0.04 (*delayed vs silenced*), P = 1 (*control vs delayed*).

Europe PMC Funders Author Manuscripts

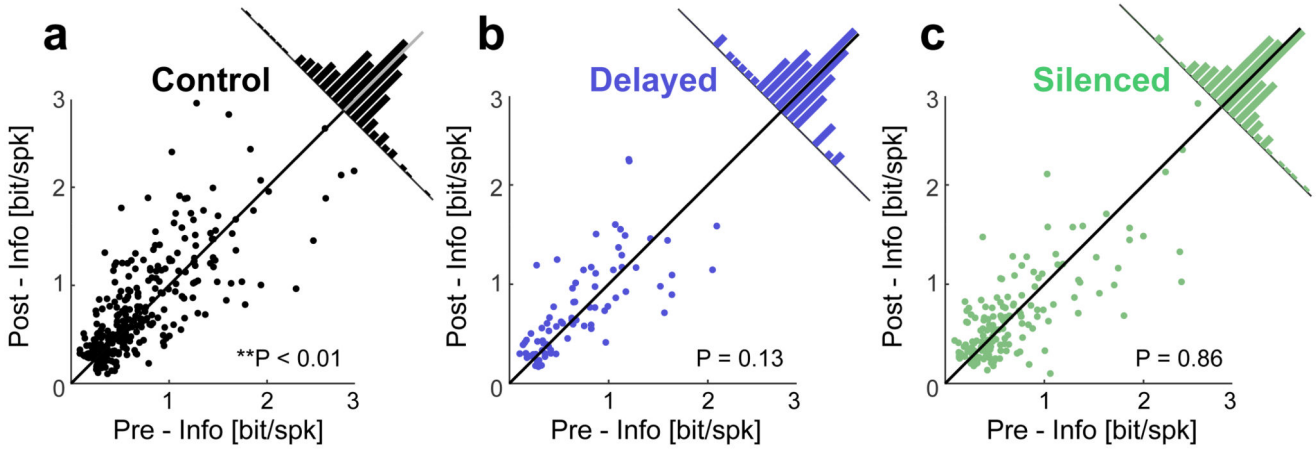

Figure 4. SPW-R silencing impact information measures of place cells.

(a-c) Distributions of "information content" values carried by place cells during pre- and post-learning exploration epochs. The information content of *silenced* place cells (c) remained similar across pre- and post-learning exploration epochs (0.68 ± 0.04 and 0.67 ± 0.04 bit/spk for pre and post, respectively; Wilcoxon's paired signed rank test: P = 0.86; n = 167 SPW-R *silenced* place cells) while *control* place cells (a) showed an increased information content (*control* group: 0.74 ± 0.03 and 0.80 ± 0.03 bit/spk for pre and post, respectively; *delayed* group: 0.70 ± 0.05 and 0.75 ± 0.05 bit/spk; P = 0.007, P = 0.13 for *control* and *delayed* groups, respectively; n = 283 control, n = 81 delayed silenced place cells). Two outlier values in the *silenced* and *control* groups are not displayed but included in the statistical analyses (their exclusion does not affect the conclusions).

Europe PMC Funders Author Manuscripts

Europe PMC Funders Author Manuscripts

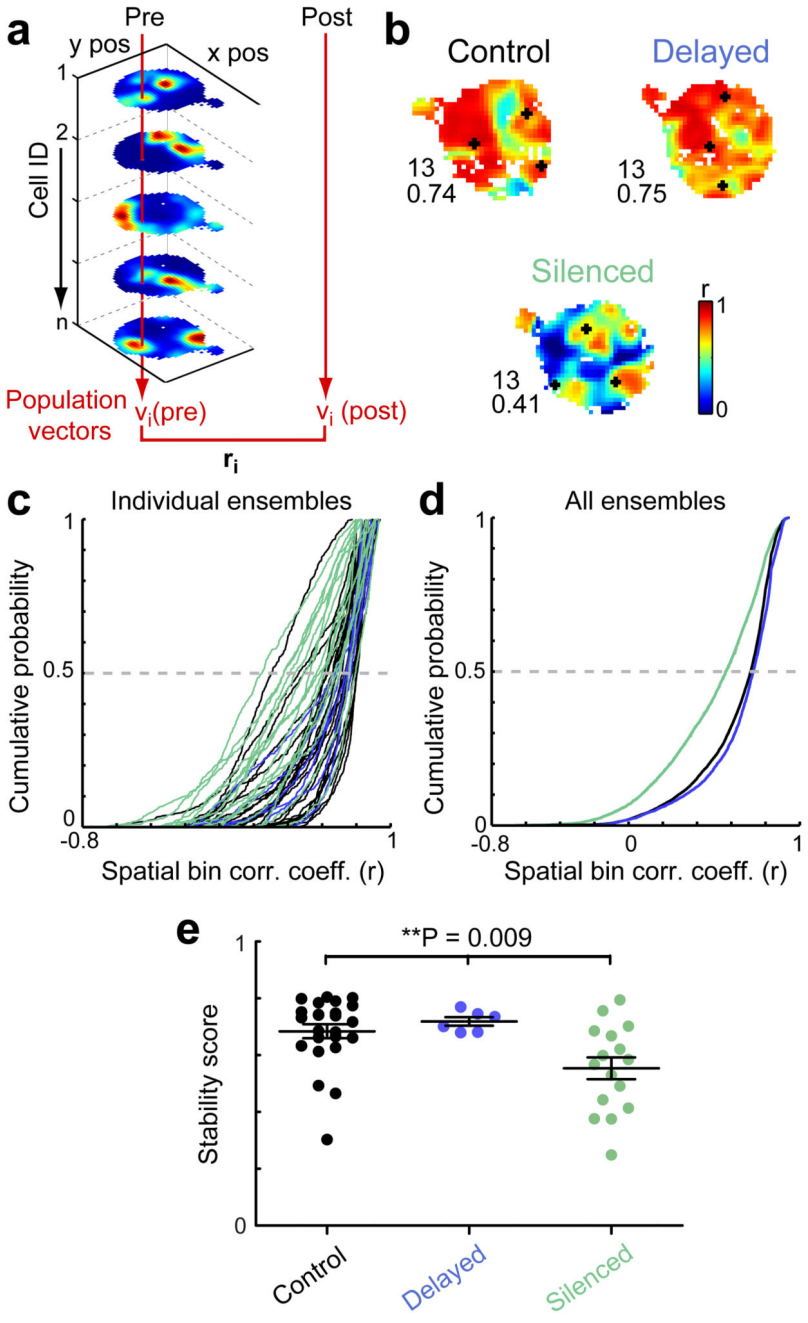

Figure 5. Silencing neurons during SPW-Rs impairs place map stability of place cell ensembles.

(a) Schematic illustrating population vector analysis method. For each spatial bin *i*, a population vector v_i was constructed containing the rates in the bin *i* of each cell of the ensemble. This was done for all spatial bins, separately for the rate maps of the pre- and post-learning exploration epochs. Then, for each spatial bin *i*, the Pearson correlation (r_i) between v_i(pre) and v_i(post) was computed. r_i indicates the stability of the ensemble spatial representation at pixel *i*. Correlation maps were constructed by assigning the r values to their respective positions in x and y. **(b)** Examples of correlation maps obtained for ensembles of

control, *delayed* and *silenced* place cells. Correlation values of individual spatial bins (r) are color coded. The number of cells part of the ensemble and the stability score, defined as the median of all bins' correlation values (r), are indicated on the left of each map. Goal locations are indicated by black crosses. **(c)** Cumulative distribution of population correlation values across spatial bins for individual ensembles of place cells. n = 24 *control* (black), 6 *delayed* (blue) and 16 *silenced* ensembles of place cells (green). **(d)** Cumulative distributions of the correlation values accumulated for all ensembles of place cells from the three groups. **(e)** Stability scores for the individual ensembles of place cells shown in (c). Kruskall Wallis test: **P = 0.009; Tukey's *post-hoc* tests: *P = 0.013 (control *vs* silenced), P = 0.94 (control *vs* delayed), P = 0.068 (delayed *vs* silenced).

Europe PMC Funders Author Manuscripts

Europe PMC Funders Author Manuscripts

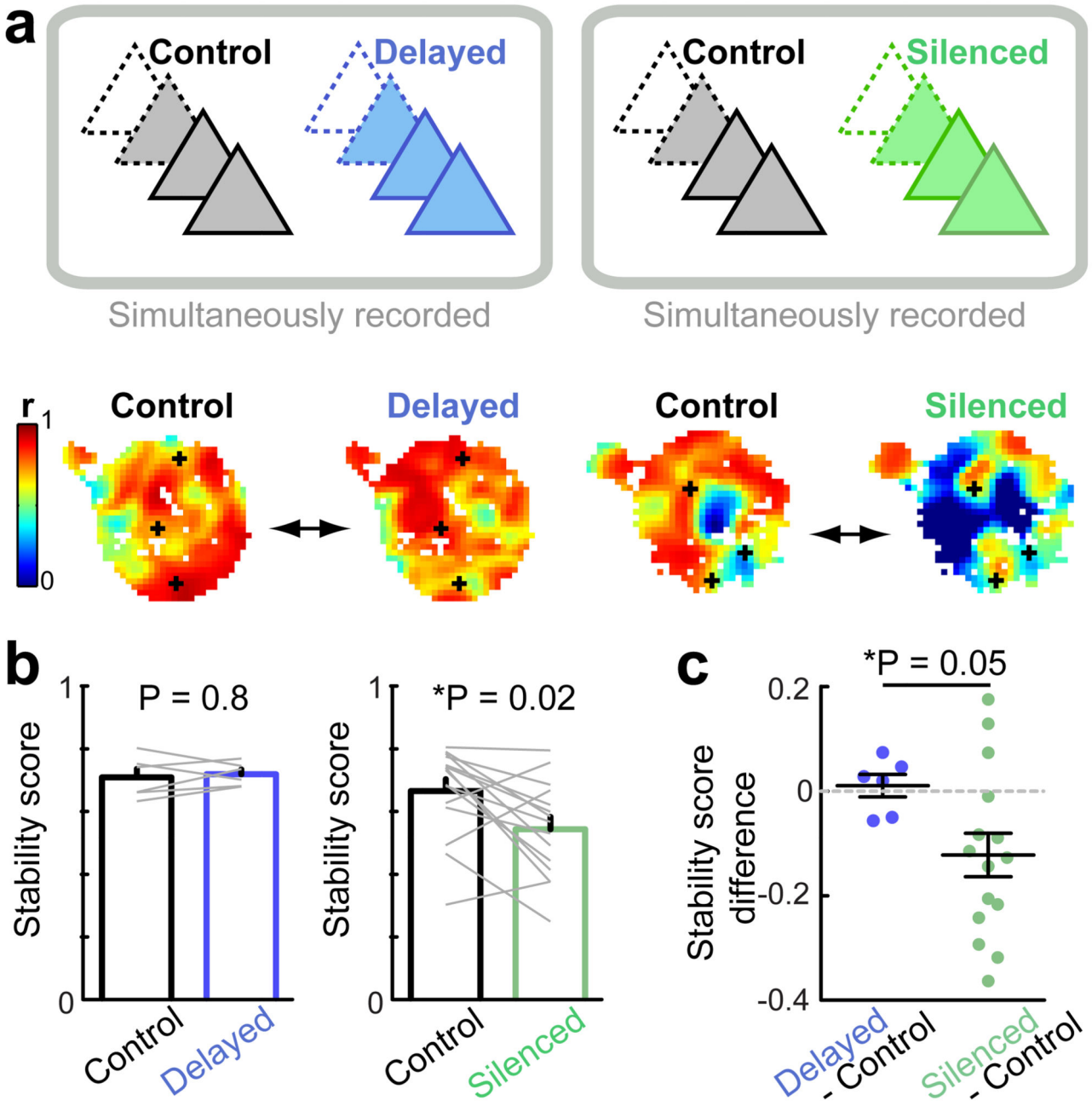

Figure 6. SPW-R silenced ensembles of place cells show destabilized spatial representation as compared to simultaneously recorded control ensembles.

(a) Top: Schematic illustrating the method used for within-session comparison of place cell ensemble pairs. Bottom: Examples of correlation maps for pairs of ensembles, simultaneously recorded within the same session (left, ensembles of *control* and *delayed* place cells; right, ensembles of *control* and *silenced* place cells) **(b)** Left: Ensembles of *delayed* place cells show similar stability scores to their matched *control* from the same recording session (score: 0.71 ± 0.03 and 0.72 ± 0.02 for *control* and *delayed* ensembles,

respectively; Wilcoxon's paired signed rank test: P = 0.84, n = 6 pairs). Right: In contrast, ensembles of *silenced* place cells show a lower stability score compared to their matched *control* ensembles (score: 0.67 ± 0.04 and 0.54 ± 0.04 for *control* and *silenced* ensembles, respectively; *P = 0.015, n = 15 pairs). **(c)** Within-session differences between the stability scores of optogenetically manipulated ensembles and their matched control ensembles (0.01 ± 0.02 for *delayed-control* pairs and -0.12 ± 0.04 for *silenced-control* pairs). Mann-Whitney U test: *P = 0.047. Dashed grey line indicates zero level (no difference).

Europe PMC Funders Author Manuscripts

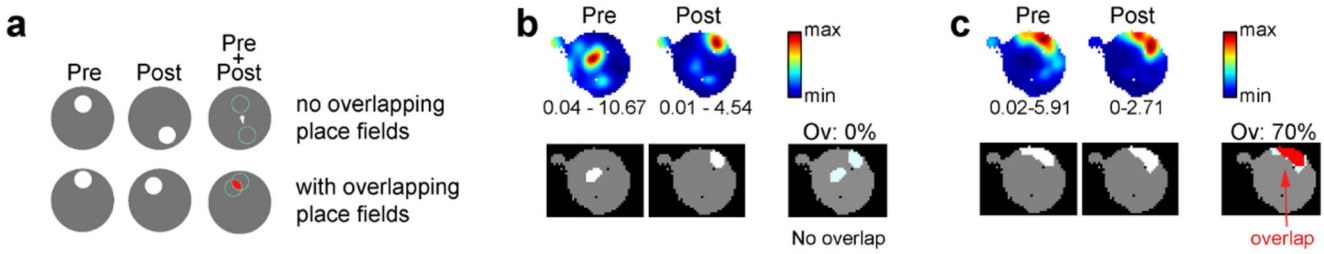

Method Figure 1. Place field overlap calculation method and examples.

a. Schematic illustrating the method used to compute place field overlap for a place cell with non-overlapping place fields (top) and a place cell with overlapping place fields (bottom). b-c. Examples of place cells with non-overlapping (b) and overlapping (c) place fields. Firing rate maps are shown for the pre- and post-exploration epochs (top; minimum and maximum rates are indicated below each map) with their corresponding detected place fields (white areas) below. The sum of the 'pre' and 'post' place fields, with (b) or without (b) overlap (red), is depicted on the right.

Europe PMC Funders Author Manuscripts